

## EVALUATION OF FLUID FLOW IN HYDRO GENERATOR THROUGH COMPUTATIONAL FLUID DYNAMICS USING ANSYS CFX

**Danilo de Souza Braga, danilo\_brg@hotmail.com**

**Adry Kleber Ferreira Lima, aee\_adry@hotmail.com**

Universidade Federal do Pará – UFPA – Faculdade de Engenharia Mecânica – Campus Universitário do Guamá – CEP: 66075-900 – Belém – Pará – Brasil

**Newton Sure Soeiro, nsoeiro@ufpa.br**

Universidade Federal do Pará – UFPA – Faculdade de Engenharia Mecânica – Campus Universitário do Guamá – CEP: 66075-900 – Belém – Pará – Brasil

**Marcos Antônio Feitosa da Silva, marcosfeitosa@eln.gov.br**

Centro de tecnologia da Eletronorte - Centrais Elétricas do Norte do Brasil S.A - Rodovia Arthur Bernardes, 2300 – Miramar – CEP: 66119-010– Belém – Pará – Brasil

**Jacques Philippe Marcel Sanz, Jacques, Sanz@eletronorte.gov.br**

Centro de tecnologia da Eletronorte - Centrais Elétricas do Norte do Brasil S.A - Rodovia Arthur Bernardes, 2300 – Miramar – CEP: 66119-010– Belém – Pará – Brasil

**Abstract.** *At Brazil, the generation of electrical energy from the available water resources is significant. This generation process can be based on the use of hydro generator, which is made up of an electric generator and turbine, and this turbine unit that converts hydraulic energy into mechanical energy, which is converted into electrical energy in the generator. This paper presents a numerical modeling, based on computational fluid dynamics (CFD) using the ANSYS CFX® for simulation hydro generator in operation at a generating unit located on north Brazil, where the hydrodynamic behavior of the set is determined, especially on volute, pre-guide vanes, turbine and duct suction. The results allow us to deduce that the phenomena arise from the hydraulic flow in each component, providing valuable information about the performance of hydro generator working in adverse operating conditions. The model results are validated from parameter information obtained by sensors installed in the components of the hydro generator.*

**Keywords:** *Finite Volume Method, Computational Fluid Dynamics, Flow on hydro generators*

### 1. INTRODUCTION

Certainly, the hydro generator is one of the most important equipment of hydroelectric plants, these equipments are essential in the energy generation process and therefore deserves special attention from manufacturers, technicians and researchers about the proper functioning and, consequently, it is operational availability. Another important fact about these equipments are designed to have very long lifetime, however it is necessary to monitor the characteristics hydraulic, which vary with time of operation. Thus, it becomes important to understand and predict the hydrodynamic behavior, related to this equipment, to keep it security, reliability and operational availability.

The hydrodynamic analysis of a Francis turbine type is an important tool for evaluating operational and structural conditions of these units, using construction techniques of numerical models, which will provide knowledge of causes of failures, giving enough allowance for technicians to diagnose emerging defects and, thus, protect all the equipment against large losses.

In the analysis discussed throughout this article will be used the finite volume method (FVM), which will be used ANSYS CFX software for numerical simulations of fluid flow through the main components of the turbine: the spiral casing, runner and draft tube. Thus, allowing extracting the fields of pressure, velocity and hydrodynamic force, where these ones are sources of hydroelectric power excitation of structural components of hydro generator.

In the technical literature related to the problems in hydro generator is large of important information. Barbosa (1991) developed a study of core vortex in Francis turbine, aiming to predict the frequency of vortex in the design of the machine. This type of oscillatory phenomenon cause recurring problems such as: loss of turbine efficiency, structural failure of turbines, generators and foundations of the mill, as well as, potential fluctuations in the units.

Santos et al. (2002) presented a numerical study of turbulent flow through a turbine type bulb. The machine was simulated from the water outlet, through the guide vanes, rotor and draft tube. The simulations were performed with the software ANSYS CFX. For comparison the simulated machine was disengaged and engaged, wherever the final results were quite similar.

Kruger et al. (2007) investigated the fluid flow in a Francis turbine, using the method of finite volume. The goal was to evaluate the regions of cavitation by pressure steaming analysis, besides knowing the fluid flow inside the turbine. The study is very importance for understanding the behavior of the fluid in the turbine blades and identifying regions of cavitations.

This paper presents a numerical modeling based on finite volume method to simulate the conditions of the working fluid passing through a unit of hydro power plant of Tucuruí, located in the municipality of Tucuruí, in Pará state.

## 2. METHODOLOGY

The Figure 1 represents a synthesis methodology of how this work is structured. Thus, initially we have the knowledge of the physical problem, and then, a conception of the mathematical model, which is submitted to the steps of simulation, summarized in preprocessing, solution (or analysis) and post-processing is that the end of this last step we obtain the results in this case referring to the flow of fluid, which should be calibrated in order to validate the numerical model.

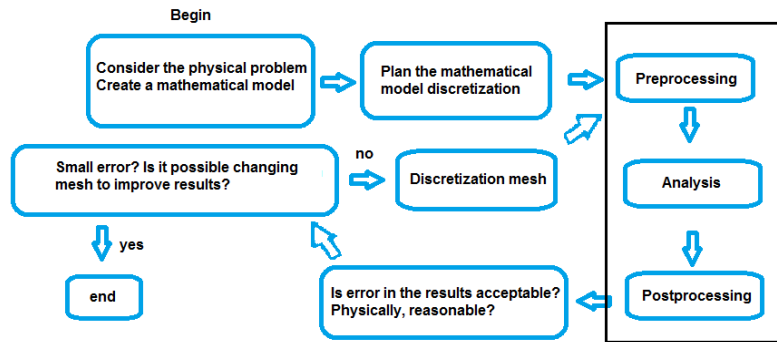


Figure 1: Flowchart depicting the modeling process.

## 3. NUMERICAL MODELING

In power plants, the working fluid is of fundamental importance for power generation. However, the flow of fluid through various components of the turbine must be controlled, otherwise it may result in appearance some severity that can cause dynamic imbalance in the hydro generator, such as: cavitation, vortex core intensification and amplification of the hydraulic loads. For this purpose, numerical studies show the method of finite volume, as the most suitable to represent these effects. Using this method, with the support of experimental data used in procedure validating models, enables phenomena understanding associated with the real problem, in most cases, good precision and economic viability, urging of science and industry.

### 3.1. Equations from CFD to problem solution

The equation 1 and 2 used to determine the pressure fields and velocity of the fluid flow inside as the turbine were the equations of continuity, momentum and Navier-Stokes.

$$\nabla \cdot \vec{U} = 0 \quad (1)$$

$$\frac{\partial(\rho U)}{\partial t} + \nabla \cdot (\rho U \otimes U) = -\nabla P + \nabla \cdot [\mu(\nabla U + \nabla U^T)] + \rho g \quad (2)$$

Where,  $\rho$  is the density,  $P$  is the static pressure,  $\mu$  is the dynamic viscosity,  $U$  is the velocity e  $g$  is the gravity acceleration.

These equations are valid for isotropic fluids, incompressible and of constant viscosity, whose application is determining the pressure and velocity at any point. However, it is emphasize that these equations are not solvable analytically, only with computational tools can get the solutions of these equations. One method of solution is the FVM (finite volume method), which will be used to develop these equations. This method has been presented, currently, as the best numerical method for solution of these equations.

### 3.2. Turbulence model

The turbulence model (k- $\epsilon$ ) has provided good results for numerical models involving turbulence and because it has good strength in the solutions of the equations of fluid transport property (pressure and velocity). This model is semi-empirical equation, based on transport equations of turbulent kinetic energy (k) and its viscous dissipation rate ( $\epsilon$ ). The turbulent kinetic energy and viscous dissipation are obtained, respectively, by the transport equations that follow:

Transport equation for turbulent kinetic energy,  $k$ :

$$\rho \frac{\partial k}{\partial t} + \rho \bar{u}_j \frac{\partial k}{\partial x_j} = \frac{\partial}{\partial x_j} \left( \left( \mu + \frac{\mu_t}{\sigma_k} \right) \frac{\partial k}{\partial x_j} \right) + \overline{\rho u_j' u_l'} \frac{\partial \bar{u}_l}{\partial x_j} - \rho \epsilon \quad (3)$$

Equation for viscous dissipation rate,  $\epsilon$ :

$$\rho \frac{\partial \epsilon}{\partial t} + \rho \bar{u}_j \frac{\partial \epsilon}{\partial x_j} = \frac{\partial}{\partial x_j} \left( \left( \mu + \frac{\mu_t}{\sigma_\epsilon} \right) \frac{\partial \epsilon}{\partial x_j} \right) + C_{\epsilon 1} \frac{\epsilon}{k} \left( \overline{\rho u_j' u_l'} \frac{\partial \bar{u}_l}{\partial x_j} \right) - C_{\epsilon 2} \rho \frac{\epsilon^2}{k} \quad (4)$$

Where,  $C_{\epsilon 1}$ ,  $C_{\epsilon 2}$ ,  $\sigma_k$  e  $\sigma_\epsilon$  are Prandtl's turbulent variables ( $k$ ) e ( $\epsilon$ ), with constant values:  $C_{\epsilon 1} = 1,44$ ,  $C_{\epsilon 2} = 1,92$ ,  $\sigma_k = 1,0$  e  $\sigma_\epsilon = 1,3$  and  $\mu_t$  is turbulent viscosity.

### 3.3. Boundary conditions

All the CFD problems are defined in initial values and boundary values. It is important to correlate and understand how they relate to modeling with greater approximation of the real models. The implementation of boundary conditions in a mathematical problem simplifies and automates all numerical analysis. For fluid flow, we can establish the following conditions at the borders of the volumes of controls: inlet, outlet and wall conditions.

#### 3.3.1. Inlet boundary conditions

According Malalasekera (1995), inlet boundary condition from a numeric domain defined by all the variables necessary to determine the flow in that region inlet domain. For example, in Figure 2, there is a particular case where the flow occurs in the  $x$  direction (horizontal direction). The grid arrangement determines the field immediately after the inlet region, which gives the determination of  $u$ -momentum. The direction of flow is taken predominantly from left to right. Therefore, the nodes of the line  $I = 1$  (or  $i = 2$ ) are used to determine inlet values of flow variables (indicated by  $u_{in}$ ), in other words, the discretization equations are solved only from nodes of the subsequent line.

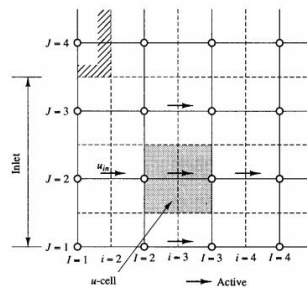


Figure 2:  $u$ -velocity cell at the inlet boundary. (Source: Malalasekera (1995))

#### 3.3.2. Outlet boundary conditions

The outlet conditions can be used in conjunction with inlet conditions. If outlet location is significantly away from the flow geometry studied frequently enough to be fully developed, where there is no change in the flow direction. In the Figure 3, there is a grid arrangement near an exit condition. This arrangement determines domain just before leaving. In the region shaded is applied to a surface and outlet state in which the gradients of all variable, with possible exception of pressure, are zero in the direction of flow. Thus, it is usually possible to predict them reasonably to the flow direction at a great distance from the obstacle.

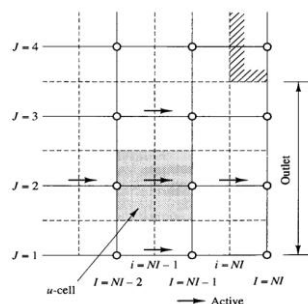


Figure 3: u-velocity cell at an outlet boundary. (Source: Malalasekera (1995))

### 3.3.3. Wall boundary conditions

The boundary conditions for the wall are the most likely to be seen in confined flows. This condition can be divided into two other types: wall-slip condition and no-slip. The non-slip condition is assumed that the fluid in contact with the wall, get the same speed. The fluid particles closest to the wall are slowed down and if the wall is impermeable to speed will be zero. The most common example is the flow over a flat plate. In the case of the sliding condition, the wall is impermeable, but it is considered that there is no friction between the fluid and the wall. For example, a supersonic flow.

### 3.4. Preprocessing stage

This step will be described the process of creating a numerical model of each component of the Francis turbine, and definition of the mesh to be used in each model.

#### 3.4.1 Construction of the geometric model

The main components that contribute to the transformation of hydro energy to kinetic energy of rotation are: spiral casing, stay vanes, runner and draft tube. These elements must be modeled in order to use the methodological approach highlighted earlier.

In table 1 shows main characteristics of Francis turbine the number one of hydro power plant of Tucuruí-PA.

Table 1: Characteristics of hydraulic turbine

Turbine	
Type	Francis
Blade number	12
Power	360 MW
Head Available	66 m
Mass Flow	597 m <sup>3</sup> /s
Specific speed	295,4 rpm
Start speed	170 rpm
Nominal speed	81,8 rpm

\*Source: Report of failure or defect in equipment (ELETRONORTE), fl.01/20, 1986

The geometric information from of the components of hydro generator, provided by Eletronorte, it was the use of CAD platform for obtaining real-scale geometry of each component, such that they preserve the maximum possible fidelity, as can be seen in Figure 4.

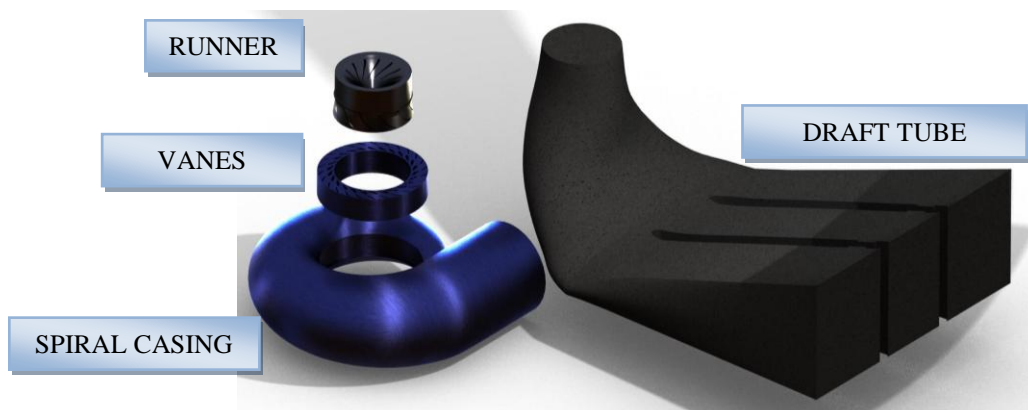


Figure 4: Geometry of the main components of the hydraulic turbine used in the simulation.

#### 3.4.2 Definition of the finite volumes mesh

The mesh creation is initial step to be defined in a simulation. The mesh quality definition is directly reflects in accuracy of results, and facilitate convergence of the model. The software used for creating the mesh of finite volumes was the CFX - Mesh, available in package Ansys Workbench 11.0. This software uses tetrahedral, prismatic, hexahedral

and pyramidal elements to mesh generation.

The mesh creation of geometrical model was done with the uncoupled components, wherever, we was taken into consideration the complexity of each of the components involved in the study, thus, enabling to obtain refined mesh in perfect agreement with the peculiarities of each component. Figure 5 shows the mesh used in modeling, with their respective characteristics.

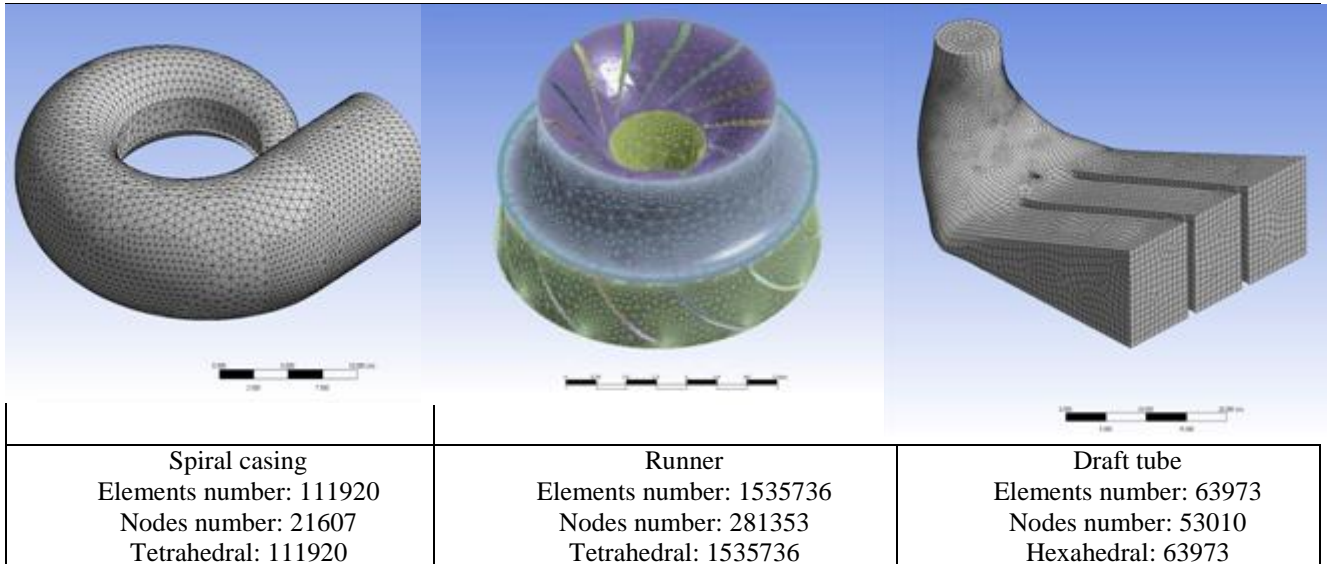


Figure 5: Computational domains in finite volume.

The mesh size from each component of the turbine, the next step is to equate each control volume mesh created by the software. If mesh is very refined has more than one dimension, number of control volumes increases stress on computational recourse. According to Maliska (1995), procedure should be: take stock of the property to the border volumes are using the boundary conditions.

### 3.5. Solution stage

#### 3.5.1. Boundary conditions

For this analysis, the parameters are directly involved velocity and pressure. Therefore, boundary conditions sets are more stable: mass flow inlet, or velocity, and static pressure in the output, followed by total pressure at the input and velocity in outlet, or mass flow. Thus, there are:

Inlet: The inlet condition was defined mass flow, which is determined by mass flow through the cross section of the input of the spiral, from the equation 5:

$$Q_{inlet} = v_{spiral-casing} * \frac{\Pi d_{spiral-casing}^2}{4} \quad (5)$$

Wherever  $v$  is inlet velocity into the spiral casing e  $d_{spiral-casing}$  input diameter of the spiral casing.

Wall: This boundary condition is common along the containment model in parts of the flowing fluid. Among the boundary conditions of type wall that represents the best option in the runoff constituent parts of the turbine is no slip. This option is accepted that the velocity near the wall is zero, in other words,  $U_{wall} = 0$ .

Interface: The interface condition between domains represents the transition region between them, becoming then the surface of intersection of the areas involved. For this case, these regions are very important because there is no connection between static and rotating domains, causing major disruption in the flow, consequently results in changes in focus.

Outlet: The hydrostatic pressure was inserted into the model for the boundary outlet condition domain of draft tube. This depends upon value head available. The values entered into numerical model were extracted from RT074702006 technical report, conducted by the Center for Technology ELETRONORTE. The pressure at the outlet of the draft tube is specified for a drop of 66m.

For each opening condition of the guide vanes were inserted into the numerical models of flow values relative to the opening. These data were extracted from reports “the index test”, thereby enabling the realization computational simulations in different operating conditions. The graph in Figure 6 was constructed from the values of opening and

mass flow extracted from the trials of "the index test", showing behavior of flow in different openings of the vanes and head available.

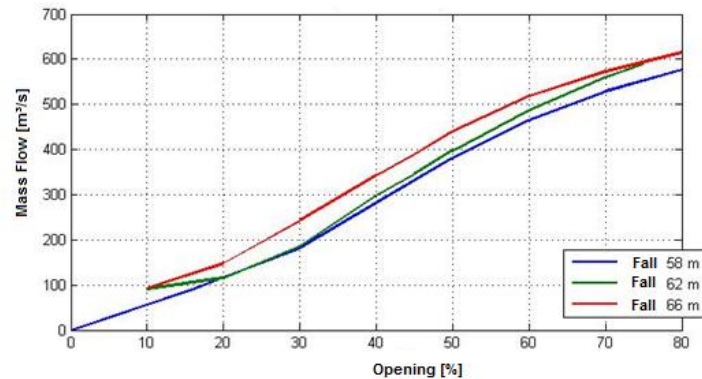


Figure 6: Mass flow versus opening of the vanes in different crude falls.

#### 4. RESULT AND DISCURSSION

In this paper, simulations were performed only for the opening of 50% of the guide vanes. Keeping the crude fall 62m, because this fall that implies greater severity for the operating conditions and also has the greatest number of favorable information to the calibration of the model. However, the biggest fall recorded in technical reports ELETRONORTE is 66m, which is reached only for performing the index test, as noted in the INDEX TEST, 29/11/1986. In this fall has been the most critical conditions for the operation of the machine according to intensity of the flow, however, this was not simulated because it is an unusual condition of operation, as well as a fault of experimental data needed for validation modeling.

Below are shown the results for these operating conditions, showing the pressure fields, velocity and potential regions of cavitations in hydraulic turbine each component separately, as well as some present in operation situations of the turbine to evaluate the behavior hydraulic turbine and possible severity existing in these components.

##### 4.1. Results for spiral casing

The Figure 7 shows pressure field in inlet of the spiral casing and positioning of sensors for measuring pressure, through which we can measure the consistency of the results obtained from the technical report of measurements performed by ELETRONORTE, quoted above, and therefore validity of model.

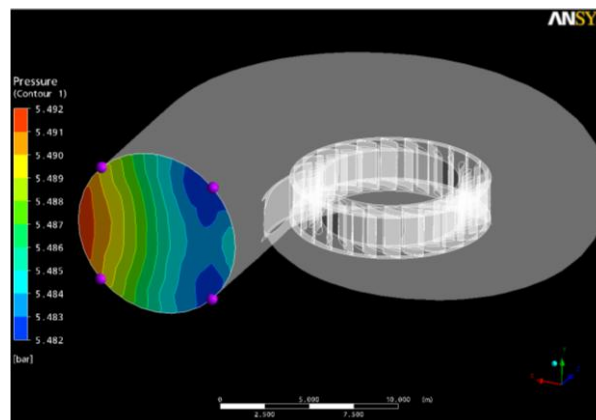


Figure 7: Pressure field inlet of the spiral casing and positioning of measuring sensors.

It is possible to see, from Figure 7, that the pressure field inlet of the spiral casing ranges from 5.482 bar and 5.492 bar, and the positioning of sensors for measuring pressure is indicated by purple spheres. For these same conditions as the experimental data show an average pressure of 5.49 bar, therefore, fully consistent with the numerical results. Observing the results shown in the previous figure, it is possible to say that it is not necessary to install and maintain four sensors for measuring the pressure inlet of the spiral casing, wherever the pressure variation at the entrance is too small and, consequently, they measure very similar values. So, it would be perfectly reasonable to believe in reducing the number of sensors, since they present a significant cost in their acquisition or maintenance.

According Maji et al (1998), hydraulic losses, in the inlet of the spiral casing and vanes outlet are even greater in some situations, in which the runner, the reduction of these losses is necessary to improve efficiency throughout the hydraulic turbine.

In Figure 8 (b), there is the pressure distribution in the imaginary plane that passes through the center of the spiral casing, this plane clearly shows the character of constant pressure along the cross section (perpendicular to this plane), an effect caused by deliberate reduction of the cross section of the spiral casing, in order to provide a incidence, the working fluid, equal to the rotor.

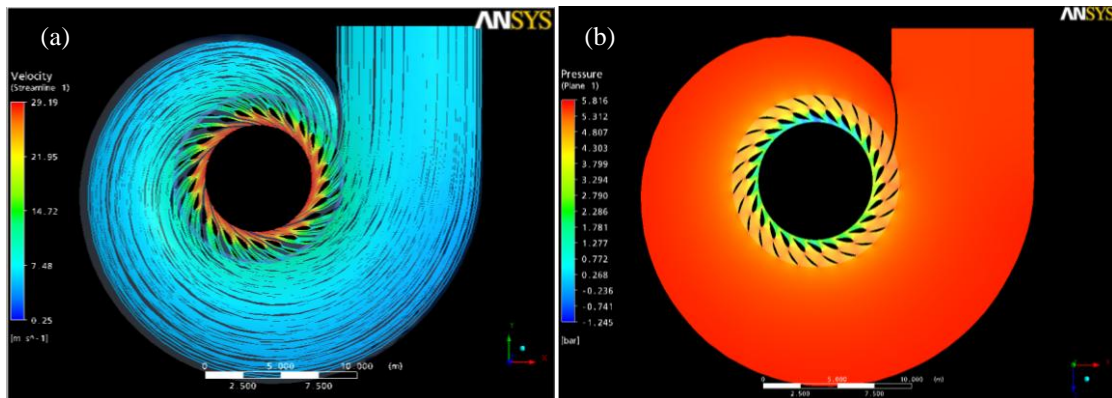


Figure 8: (a) Stream lines inside the spiral casing and magnitude of flow velocity, (b) Pressure field in the middle plane of the spiral casing.

In Figure 8 (a) we can observe the flow orderly and undisturbed (no region of significant turbulence), which is evident in the gradual increase of flow velocity, the extent to which there is an approximation of the outlet region and therefore the spiral casing inlet of the rotor. This increased velocity is intentionally caused by the spiral casing design, to maximize kinetic energy to be converted by the rotor, since this is directly proportional to the velocity of flowing fluid.

#### 4.2. Results for runner

In figure 9, we can see the pressure distribution on the blades of the rotor, and state that the most solicitude region is the external board of the blade, known as blade runner (region where the blade attaches the turbine shaft). This phenomenon can be explained by a number of factors such as the great pressure difference due the vortices formation in the frontal region of the blades, the incidence pattern of the flow and the complex geometry of it.

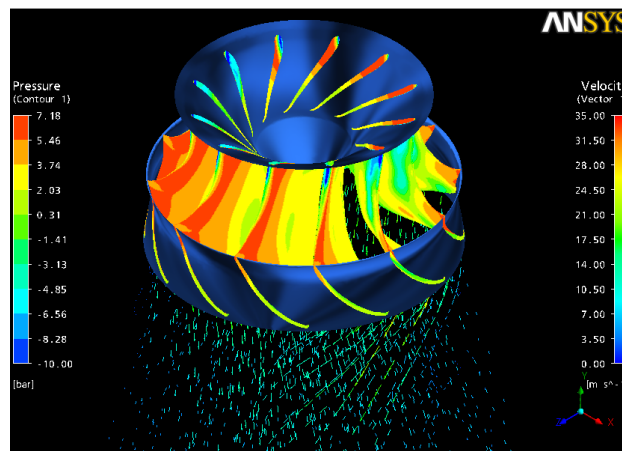


Figure 9: Pressure field on the contour of the blades and velocity vector field on the outlet of the rotor.

On the velocity vector field shown on the outlet of the rotor, one can observe a considerable reduction of the flow velocity, once we can see that the maximum value obtained is 21 m/s, less than one half of the downstream maximum

velocity, calculated as 48 m/s. We can conclude that for the situation of 50% guide vanes opened the machine presents an efficient kinetic hydraulic energy conversion.

In Figure 10 shows the regions where cavitation might occur, due the low pressure level in such regions caused by vortex formation. The pressure values decreases to a level approaching the saturation vapor pressure of water at the working temperature, causing the appearing of micro-bubbles. These micro-bubbles can implode causing the cavitation phenomenon, pitting the surface of the blades, which can remove material causing frailty on the rotor.

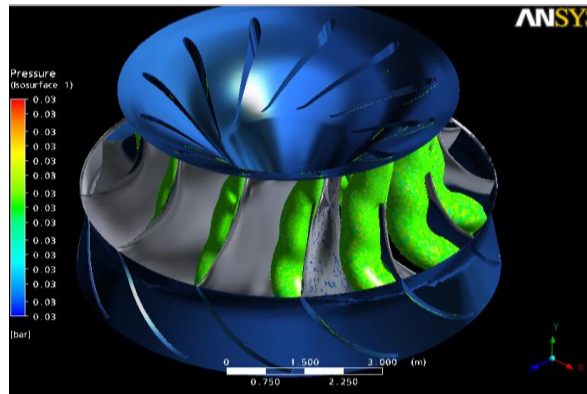


Figure 10: Possibly cavitation regions.

One of the main factors that contribute to the phenomenon of cavitation is the geometry or the constructive shape of the rotor blade, once the recirculation on the frontal region of the blade occurs due the concave shape. Other works studying this subject concluded that some changes on the rotor blade shape have significant reduction of the cavitation phenomenon, leading to a better performance and consequently reducing losses on kinetic energy conversion.

The states that phenomenon of cavitation has its origins in a number of problems on hydroelectric power plants, such: erosion of turbines, vibrations on the structure, reduction of power and efficiency, noise, etc.

#### 4.3. Results for draft tube

According to Marjavaara (2006), the efficiency of hydraulic turbines is affected significantly by the performance of the draft tube, especially at low heads and great flow rate, when subjected to elevated heads, where the hydraulic losses are considerably great.

We can observe in Figure 11 that the flow in the interior of the draft tube directs toward the draft walls at high speed, but this fact does not mean inefficiency of the rotor, rather, it increases the velocity of the fluid by its great inertia together with the rotating movement of considerably magnitude (81,8 rpm).

Another aspect is that the flow obeys a spiral pattern of the same diameter that the draft, causing the appearing of a low speed region on the center of the draft, called core vortex. According to Barbosa (1991), this low frequency phenomenon affects specially the concrete structure of the power plant, which can cause resonance, with the low frequency of exciting force originating on the vortex.

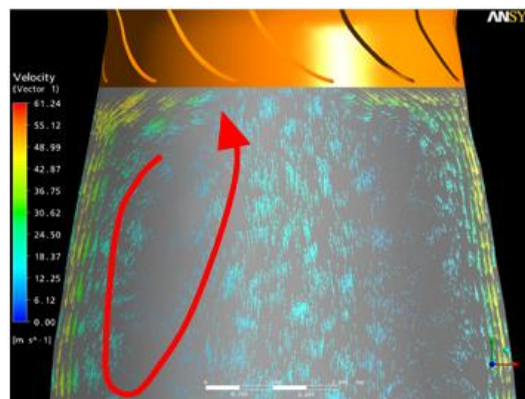


Figure 11: Vector field on the inlet of the rotor.

As shown in Figure 11, we can see the recirculation of the working fluid in a spiral pattern due the loss of flow velocity when colliding with the walls of the draft tube, and thus increasing the pressure. This fluid mass is directed to the low pressure region (next to the center of the inlet of the tube), and then returning to the rotor causing water

entrance on the wheel of the rotor (Recurrent problem reported by technicians during visits on the power plant of Tucuruí).

The development of the spiral flow on the inlet of the draft tube shows clearly accumulate of fluid on the walls of the draft, explained by the downstream velocity on the outlet of the rotor. We can also see through the vector field the expressive reduction of speed in the center of the entrance of the draft, causing a concentration of low speed mass known as “dead spot”.

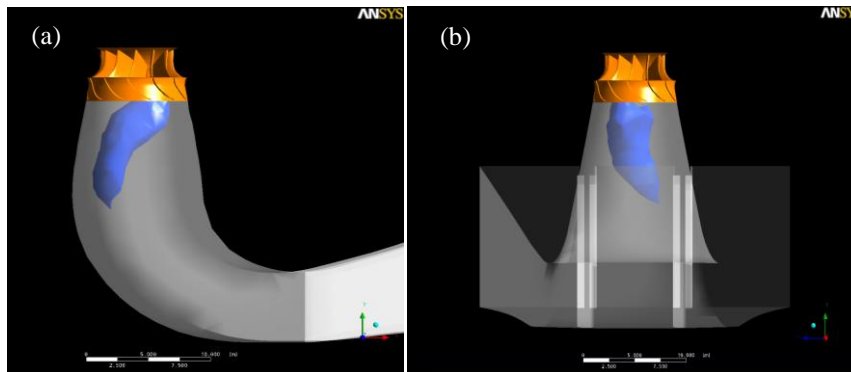


Figure 12: (a) Core vortex– lateral view (b) Core vortex– frontal view.

Figures 12 (a) and (b) show the occurrence of core vortex, caused by the “dead spot”. This phenomenon has a major importance on evaluating the machine behavior, as it presents characteristic patterns for each operating regime, thus indicating problems and anomalies occurring on the rotor or on the draft tube. According to Brandão (1987), the vortex shown on Figures 12 (a) and (b), are characteristic of this operating regime.

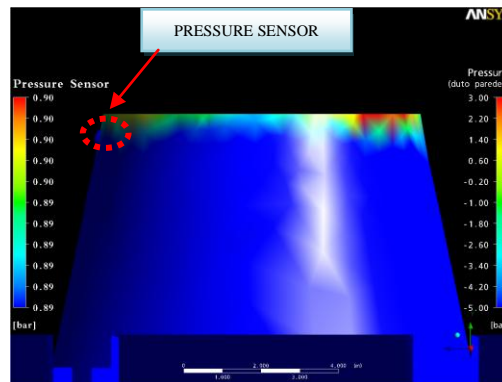


Figure 13: Positioning and sensor register of pressure on the draft tube.

According to technical reports of the “Centro de Tecnologia da Eletronorte – TCT –, dating from 31 august of 2006”, the pressure registered for the draft tube in the operating regime studied has a mean value of 0,9 bar. In this way, as we can observe in Figure 13 that the pressure obtained by the model, on the same position of the monitoring sensor is 0,89 bar, very close to the value observed in practice, so that the model is calibrated with the real system.

#### 4. CONCLUSION

The results shown in this work allow a better understanding of the machine for each opening of guide vanes, so that it is possible to analyze more efficiently the inherent operating problems. By the other side, we can conclude that no more than one sensor is necessary to monitor inlet of the spiral casing, as shown in Figures 7. It is valid to stand out that this work did not use as a parameter of validation the pressure on the turbine lid, once they were not available on the reports, for this equipment. However, the model were calibrated by using the pressures on the draft tube and on the casing, as shown early on this paper, and a possibly a reduction on the numbers of sensors on the turbine lid too.

Besides the possibility of reduction on the numbers of sensors, we can point out as another contribution of this work the mapping of the main regions where possibly cavitations would occur, as well as the origin of the problem. In this way, the mathematical model developed is useful helping maintenance inspections on the blades of the rotor, and on decision making in the sense of minimize the harmful cavitations effects. The phenomena of cavitations and vortices, according to Aschenbrenner et al (2006), limit the operating regime of Francis turbines and generally take place on draft

tubes and rotor of the turbine. These phenomena happen when the turbine operates on partial charge, or overcharge, causing fluctuating pressures.

## 5. ACKNOWLEDGEMENTS

Centrais Elétricas do Norte do Brasil S.A – Eletronorte, by proportioning a period of convivence with its technical staff, which was of great value to our professional development.

## 6. REFERENCES

Aschenbrenner, T.; Moser, W.; Otto, A. “Classification of Vortex and Cavitation Phenomena and Assessment of CFD Prediction Capabilities”. Artigo apresentado no 23 rd IAHR Symposium, Japão, 2006.

Barbosa, A. A., 1991. “Vórtice de Núcleo em Turbinas Francis – Estudo teórico Experimental”. Dissertação de mestrado – Escola Federal de Itajubá, MG, pp. 94.

Kruger, M.; Ataídes, R., Kessler, M., Cordeiro, P. T. R. A., 2008. “Numerical Study of Fluid Flow in a Francis Turbine”. In: 24th Symposium on Hydraulic Machinery and Systems – IAHR, Foz do Iguaçu – PR.

Maji, P. K., 1998. “Three-dimensional Analysis of Flow in Spiral Casing of a Reaction Turbine Using a Differently Weighted Petrov Galerkin Method”. Jornal – Elsevier Science Ltda.

Maliska, C.R., 1995. “Transferência de Calor e Mecânica do Flúidos Computacional”. LTC - Livros Técnicos e Científicos. Rio de Janeiro, Brasil. pp. 75 – 152.

Marjavaara, B. D., 2006 “CFD driven optimization of hydraulic turbine draft tubes using surrgate models”. Doctoral thesis – Luleå University, Luleå, pp. 402.

Santos, C. C. B., Coelho, J. G.; Junior, A. C. P. B, 2002. “Estudo Numérico de uma Turbina Hidráulica do Tipo Bulbo”. Universidade de Brasília. 16° POSMEC, Uberlândia-MG, Paper.

Versteeg, H. K., Malalasekera, W., 1995. “An introduction to computational fluid dynamics the finite volume method”. Ed. Longman Group Ltd. Malaysia. pp.192 – 205.

## 5. RESPONSIBILITY NOTICE

The authors are the only responsible for the printed material included in this paper.